Desalination and Water Treatment
www.deswater.com

doi:10.5004/dwt.2019.23359

139 (2019) 39–52
January

Improving the performance of air gap membrane distillation process using a developed tubular condenser compared to a flat plate condenser

Mahdi Jalayer[a], Mohammad Karimi[b,*], Seyed Mehdi Borghei[c], Amir Hessam Hassani[a]

[a]*Department of Natural Resources and Environment, Science and Research Branch, Islamic Azad University, Tehran, Iran, email: mahdi_jalayer@yahoo.com (M. Jalayer), ahhassani@srbiau.ac.ir (A.H. Hassani)*
[b]*Department of Textile Engineering, Amirkabir University of Technology, Tehran, 15914, Iran, Tel. +9821 6454 2658, email: mkarimi@aut.ac.ir (M. Karimi)*
[c]*Department of Chemical and Petroleum Engineering, Sharif University of Technology, Tehran, Iran, email: mborghei@sharif.edu (S.M. Borghei)*

Received 28 April 2018; Accepted 25 October 2018

ABSTRACT

Condensation has a considerable effect on the performance of air gap membrane distillation (AGMD) process. In this study, a novel module arrangement was successfully introduced with the aim of improving the condensation phenomena and consequently enhancing the efficiency. In this newly designed AGMD arrangement, the common flat coolant plate was replaced with several horizontal copper tubes that has been named tubular condenser. Coolant fluid was streamed inside the tubes and condensation occurred outside the tubes. To measure the performance of this new module, two types of polytetrafluoroethylen (PTFE) commercial flat sheet membranes supported by polypropylene (PP) non woven layer with different pore sizes were employed. To measure water permeation flux, laboratory prepared brackish water was introduced into the system at different temperatures, which were 40, 50, 60, 70 and 80°C. The average flux produced by the system at 80°C for a flat plate condenser with an equivalent air gap was 11.7 kg/(m^2·h); it increased up to 19.45 kg/(m^2·h) using a simple tubular condenser. To improve more, tubular condenser was developed using zigzag copper ribbons, enhancing the water permeation flux to 30.08 kg/(m^2·h). To realize the performance of developed tubular module, the effect of membrane pore size and air gap width as well as ribbons arrangement were studied.

Keywords: Membrane distillation; Performance improvement; New configuration; Tubular condenser; Flux increase

1. Introduction

Improving the efficiency of membrane distillation (MD) process as a new method of heat-based membrane separation has attracted increasing attention nowadays. Optimizing this process for desalination of sea water and brackish water is considered as an attractive replacement for the usual separation processes such as distillation and reverse osmosis processes [1–8]. In order to improve the performance of this process, different configurations have been presented. Many researchers are studying four general configurations, namely; direct contact membrane distillation (DCMD), air gap membrane distillation (AGMD), vacuum membrane distillation (VMD) and sweep gas membrane distillation (SGMD). Among these four categories, DCMD arrangement has been more popular due to the simplicity of the module and less peripheral equipment. Compared to the DCMD, the AGMD process has been used in many commercialization processes such as Memstill, Aquastil, Keple Seghers, and Scarab AB [9–14] due to many advantages such as the ability to use different cooling fluids, acceptable flux, low heat loss, and less fouling tendency [1,15–17]. Based on Alklaibi and Lior's studies [18], the thermal efficiency of the AGMD is higher by about 6% than DCMD, due to the existence of air gap. Despite various benefits, the

*Corresponding author.

flux of the ordinary flow of AGMD has been reported lower than DCMD or VMD due to the additional resistance created by the air gap [19]. Therefore, in order to increase the flux in the AGMD method, it is needed to improve the performance of the module and provide new configurations.

To increase the amount of the flux in the membrane distillation process, many efforts have been made to improve the membrane itself and its construction methods [20–25]. Along with improving the membrane, attention is paid to optimizing the process conditions in the AGMD process by Xu et al. [26]. They reported that increasing feed temperature increased permeate flux regardless of the feed concentration. Tian et al. [27] reported a significant increase in the amount of flux in the AGMD process, by changing the feed flow direction, creating rotating currents and a partial membrane contact with the cooling plate. Their results showed that the optimum partial contact area ratio is about 75–80%. Wirth and Cabassud [28] also reported improvement in flux value by changing the flow direction. They compared feed flow direction in hollow-fiber VMD module. The effect of surface roughness in counter current flow on flux quantities for the DCMD process was demonstrated by Ho et al. [29]. Up to 42.11% of the device performance enhancement was achieved for the counter current flow DCMD system in this report. The effect of liquid distributors on the performance of the VMD process was also theoretically studied by Wang et al. [30]. On the other hand, with the aim of reducing temperature polarization and improving the flux, Chernyshov et al. [31], were proposed using spacers on the AGMD method. A similar work was performed by Chu-Lin et al. [32] using several flow deflectors in DCMD process and 36% improvement of flux was reported, but a 4.2 times increase of pressure drop is encountered. CFD studies for the impact of spacer direction on the flux value were also investigated by Shakaib et al. [33]. Their simulations show that when the spacer filaments are not touching the membrane, high velocity zone at the membrane layer enhances shear stress and heat transfer rate by decreasing temperature polarization. In an other research, He et al. [34] have recommended a thermal recovery solution by intermediate stage heating of cold feed using the distillation product of the previous stage in multi-stage modules. They claimed depending on configuration (interstage heating or not) and temperature differences, recoveries of 60% and GOR values above 20 may be attainable. In addition, Yang et al. [35] investigated the effect of the using hollow fibers on the performance of DCMD in both experimental and theoretical studies. They reported a 300% improvement in the flux value. Next, Singh and Sirkar [36] introduced porous and non-porous hollow fibers to compress the volume of the module. Also, Geng et al. [37] designed a new hollow fiber module, which, by transferring the latent heat of vapors to the cold feed, improved thermal efficiency by about 80%. In addition to the AGMD arrangement, some researchers such as Winter et al. [38] reported that the creation of a third channel, based on permeate gap membrane distillation (PGMD) configuration, reduces heat loss and increases efficiency, where the third channel is added with an impenetrable foil. Also, extensive work has been done on multi-effect or multi-stage modules with improved thermal efficiency based on a combination of a cooling plate in the AGMD arrangement [39–40]. To improve overall efficiency, the latent heat of condensed vapors was used for pre-heating the feed stream by some researchers [41,42]. Chouikh et al.[43] reported a slight improvement in the amount of flux due to the movement of stagnant air in the air gap. Concerning the effect of condensation improvement on AGMD flux, Bahar et al. [44] tested two different metals as the cooling plate and showed that the flux value for the material with higher thermal conductivity was improved. Another research activity carried out for improving the condensation process to achieve higher flux employed finned surfaces. An attempt to use the finned surface to increase condensation heat transfer was introduced much earlier in the mid-1950s by Gregorig [45]. This mechanism was used extensively later to improve heat transfer in vertical fluted tubes [46–48]. In 2016, Liu et al. [49] introduced a new module called "double-pipe air gap membrane distillation" by placing a polyvinylidene fluoride (PVDF) hollow fiber membrane inside copper tubes. According to their studies, the total produced flux was 29.6 kg /m^2·h. Bahar et al. [50] used an aluminum channeled plate instead of a flat plate to improve condensation in AGMD module. They showed that the change applied to the condenser plate resulted in an improvement of about 50% in the amount of flux compared to the use of a flat cooling plate. In a similar effort, Bappy et al. [51] reported 50–58% improvement in flux values using finned cooling plates. Despite the many efforts that have been made to improve the overall performance of the AGMD module, it seems necessary to pay attention to newer configurations in the condenser section.

In this research, a tubular condenser is introduced as an alternative to the flat plate condenser to improve the amount of flux in AGMD process. For this purpose, two types of modules with two different condensers, namely tubular and flat plate, are created, then, experimental tests are carried out. In all experiments, laboratory prepared brackish water at various temperature, ranging from 40 to 80°C is pumped into the modules with different condensers and the coolant temperature was set at 20°C. Then, by adjusting the flows of hot and cold currents to 2 L/min, changes in the flux of distilled water are studied as the only variable factor in different modules. In these experiments, two types of flat sheet PTFE commercial membranes were used. With the aim of improving the performance of the new tubular condenser, the effect of using thin zigzag copper ribbons with the tubular condenser on the amount of produced flux is discussed. Besides, by calculating the equivalent air gap in the tube condenser, the performance of the new condenser is compared with a flat plate condenser. Moreover, the impact of membrane pore size, the effect of changes in the air gap width and flux variations using two membranes on both sides of the tubular condenser are analyzed.

2. Material and methods

2.1. Materials

In all experiments, laboratory prepared brackish water was used with electrical conductivity of about 4500 μS/cm. To prepare the feed solution, the sodium chloride salt of the German MERCK Corporation, with 99.5% purity was employed. This salt was dissolved in deionized water,

produced by the ABC laboratory deionized water apparatus. Two types of flat sheet membranes were used in the experiments. These hydrophobic micro-porous PTFE membranes supported by PP non woven layer were supplied by the American Membrane Solutions company. The pore size, thickness, bubble point, flow rate and other specifications of these two types of membranes are presented in Table 1. The contact angle for both types of membranes, investigated with contact angle measurement apparatus using the Sessile drop technique and liquid entry pressure (LEP) is calculated using membrane manufacturer's data.

2.2. Tubular condenser design

In the new designed condenser, ten copper tubes were used with an external diameter of 1/4 inch (D = 6.35 mm) and 0.025 inches (0.635 mm) thickness. The schematic of designed tubular condenser is illustrated in Fig. 1. According to Fig. 1, the tubes are parallel and horizontal, located at the central part of a Plexiglas sheet with a thickness of 15 mm. In addition to creating the condensation region of the system, the designed condenser also provides the required air gap in the AGMD. Coolant fluid from the designed channel is inserted into the lower part of the tube network and flows through all the tubes and after passing through the length of the tubes, goes out from the highest point on the opposite side of the condenser. The condensed vapors on the outer surface of copper tubes leave the system from the canal embedded in the bottom of the air gap section.

A simple tubular condenser is illustrated in Fig. 2a. To improve the performance of tubular condenser, thin, flexible copper ribbons of 0.2 mm thickness were used in the form of a zigzag in two modes, including three ribbons for half of the tubes, shown in Fig. 2b, and six ribbons for covering the total surface of the tubes as illustrated in Fig. 2c.

Table 1
Specifications of membranes were used in the experiments

Specification	MSPTFE022B	MSPTFE045B
Membrane media	PTFE	PTFE
Support layer	PP	PP
Pore size, µm	0.22	0.45
Wettability	Hydrophobic	Hydrophobic
Contact angle, °	130.02	129.31
Thickness, µm	170–240	170–240
Bubble point, psi	21.75–23.2	14.50–15.95
Flow rate, ml/min/cm² @ 10 psi	19–22	35–40
Liquid entry pressure (LEP), atm	8.84	4.26

2.3. Module design

In this study, three different AGMD modules presented in Fig. 3, were employed to evaluate the performance of condenser configurations. Fig. 3a illustrates the typical AGMD module with Plexiglas material. This module has two hot and cold fluid chambers on both sides, and an adjustable air gap in the middle part, along with the positions of the membrane and the condensation plate. In order to adjust the size of the air gap, rubber gaskets with different thickness, proportional to the required air gap size were used. To achieve a better mix of the fluid and avoid laminar flow in both hot and cold chambers, and to create turbulency, two plastic baffles were used in each chamber, perpendicular to the flow path. In this module, a thin copper plate of 0.2 mm thickness was used as a condensing plate. The hot fluid used in the module is laboratory prepared brackish feed water and the coolant fluid is distilled water.

In Fig. 3b, the new AGMD membrane module is shown using a tubular designed condenser. According to

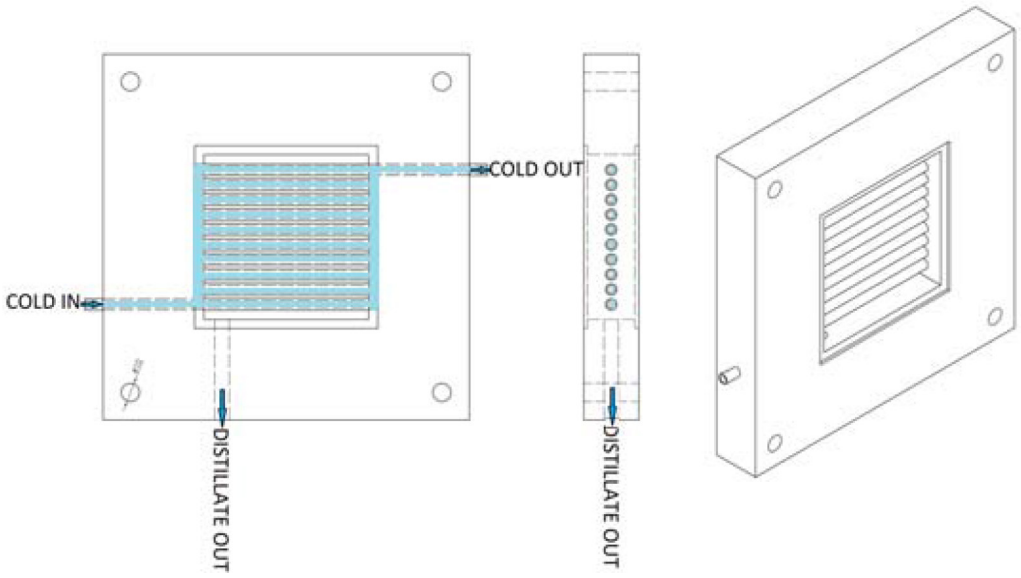

Fig. 1. Three view drawings of designed tubular condenser.

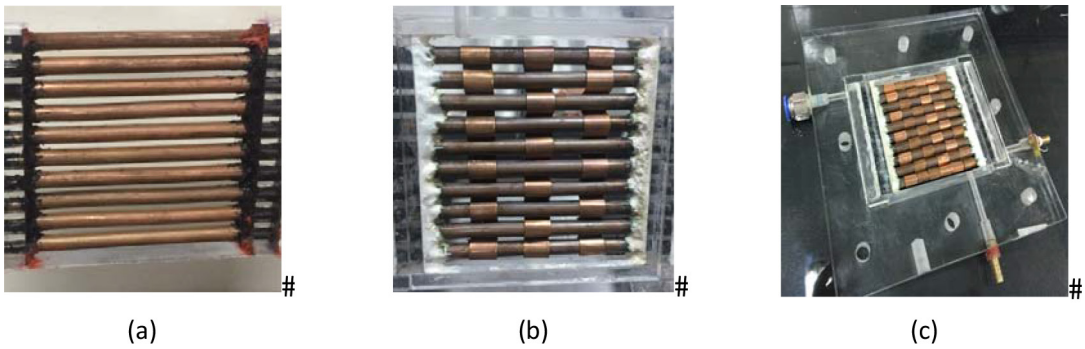

Fig. 2. Photographs of designed tubular condensers without ribbon (a) and with two modes of copper ribbons (b,c).

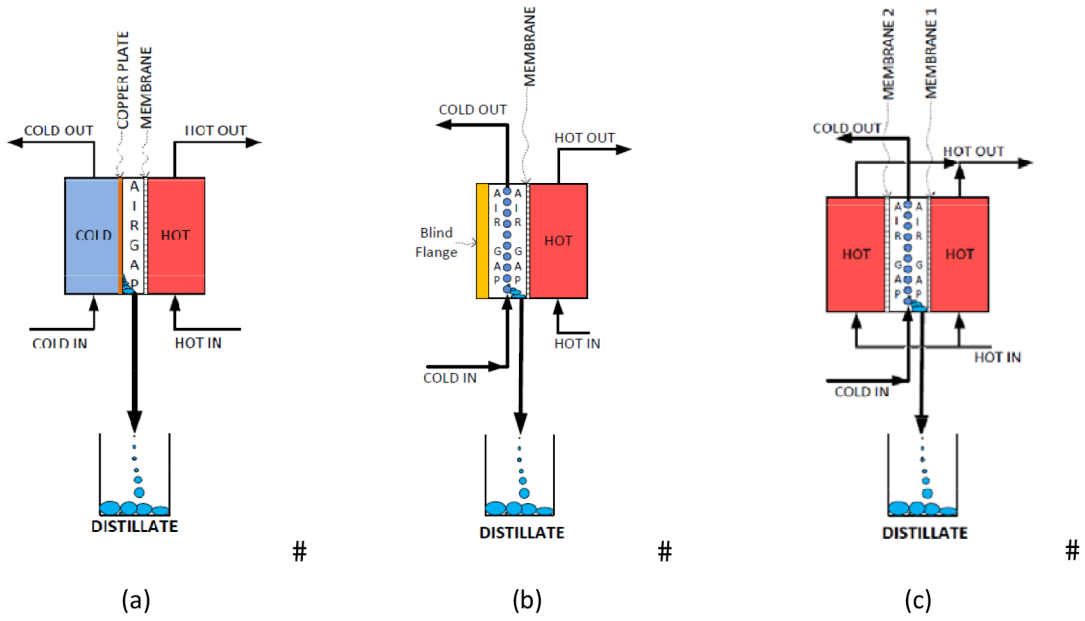

Fig. 3. Schematics of three different AGMD modules were used in the experiments.

Fig. 3b, the module includes a hot fluid chamber, a tube condenser and an air gap, as well as a blind flange for blocking the end of the air gap. The membrane is placed between the hot fluid and the condenser. The condensate generated in the condenser as the product of the process is removed from the bottom of the air gap. Cold fluid enters from the bottom of the condenser into the tube network and passes through the length of the tubes and then pulls out from the upper part. Due to the change of the condenser type from the flat plate model to tubular, it is possible to use two membranes on both sides of this condenser. Therefore, in some parts of the experiments, the module illustrated in Fig. 3c was used. Fig. 4 shows the cold and hot sides of the designed module and the position of the baffles.

2.4. Membrane distillation process

Fig. 5 illustrates the schematic of a designed lab-scale setup. In this system, a HAAKE N3 laboratory heater and a Julabo VC chiller were used. Both the heater and the chiller are temperature-adjustable with an accuracy of 0.1°C and are equipped with fluid recirculation system. In the experiments, the laboratory prepared brackish feed water was fed into the feed tank. The feed water was heated by the indirect flow of distilled water at an adjusted temperature by the heater, then was fed into the hot chamber of the module using feed pump. Pressure, flow and temperature indicators were embedded in the input and output of these sections. The fluid passes through the module's hot chamber and then returns into the feed tank. In recirculating cooling flow section, distilled water was used as coolant fluid. The cooling current temperature was regulated by the chiller and was introduced into the cold chamber by a chiller internal circulation pump. In the inlet and outlet of the cold circulation flow, the pressure, flow and temperature indicators were embedded. Lutron temperature sensors, with a precision of 0.1°C (Model: TM947), have been used in the system. The FILMTEC flow meters have been used in the range of zero to 7 L/min (with a precision of 0.5 L/min). In order to minimize the heat loss, all equipment, pipes and feed container were insulated.

In the experiments, three different modules described in the module design section (Fig. 3) were used. The

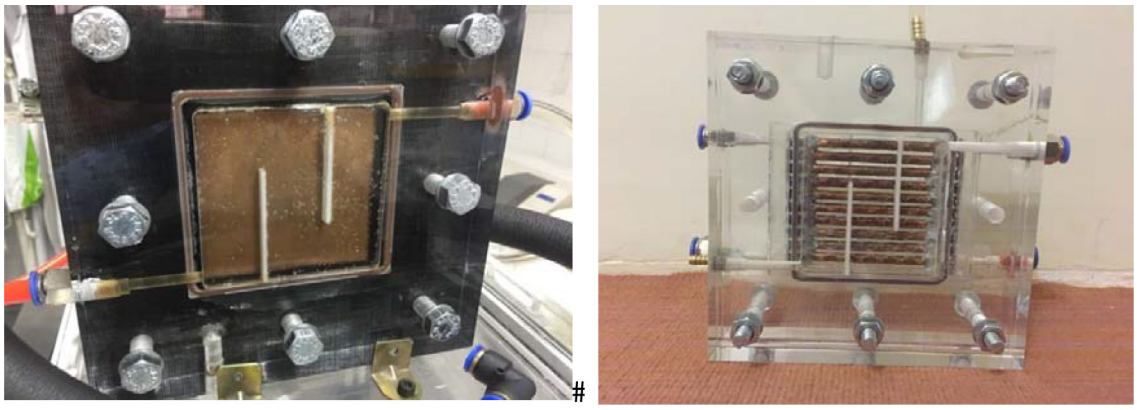

Fig. 4. Photographs of designed modules with baffles: plate condenser (a), tubular condenser (b).

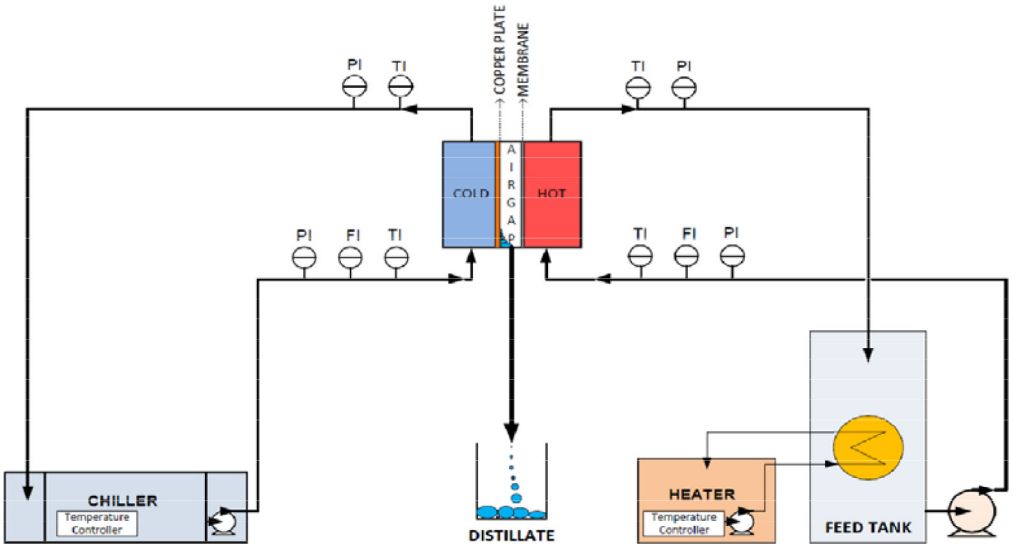

Fig. 5. Schematic of a designed lab-scale setup.

feed water was heated to the temperature of interest and entered the hot section of the module. The vapors created in the hot fluid were flowing through the membrane and after entering the air gap were condensed on the copper plate or outside surface of the tubes, depending on the type of condenser of each module. The distilled water from the path that was made in the lower part of the air gap goes out gravitationally. The distilled water is collected in the container and weighed consecutively. A AND (model EK6100i) digital balance was used to measure the distilled water production rate, with an accuracy of 0.1 g. The output of this balance can be recorded on the computer by the software at one second intervals. To calculate the flux in kilograms per square meter per hour, the area of the membrane used in the module is specified. Also the quantity of distilled water produced in kilograms was recorded in the balance at a fixed time interval. In different experiments, Hand Held 8306 portable conductivity transmitter was used to control the electrical conductivity of the distilled water as a criterion of membrane performance.

2.5. Equivalent air gap in tubular condenser

Fig. 6 indicates the air gap where a vapor molecule will be traversed to reach the condensation point in three modes using a flat plate condenser in Fig. 6a, tubular condenser with a membrane in Fig. 6b, and a tubular condenser with two membranes in Fig. 6c. When using a flat plate condenser and the vapor passing through the membrane, molecule A in Fig. 6a, traverses the air gap width and reaches the condensation plate. But in the case of the tubular condenser, the surface of the tubes as the point of condensation is not flat, but an arch, and thus vapors passing through the membrane are closer to the condensation point in some places and in other places are more distant from the condensation point. For example, in Fig. 6b, molecule A, traverses the shortest path to reach the condensation point and molecule B has a longer path than molecule A, while the molecule C passes through it without colliding with the condenser tubes. This molecule will probably collide with one of the tubes on the return path. In Fig. 6c, due to the use of two membranes on both sides, the vapor molecules will

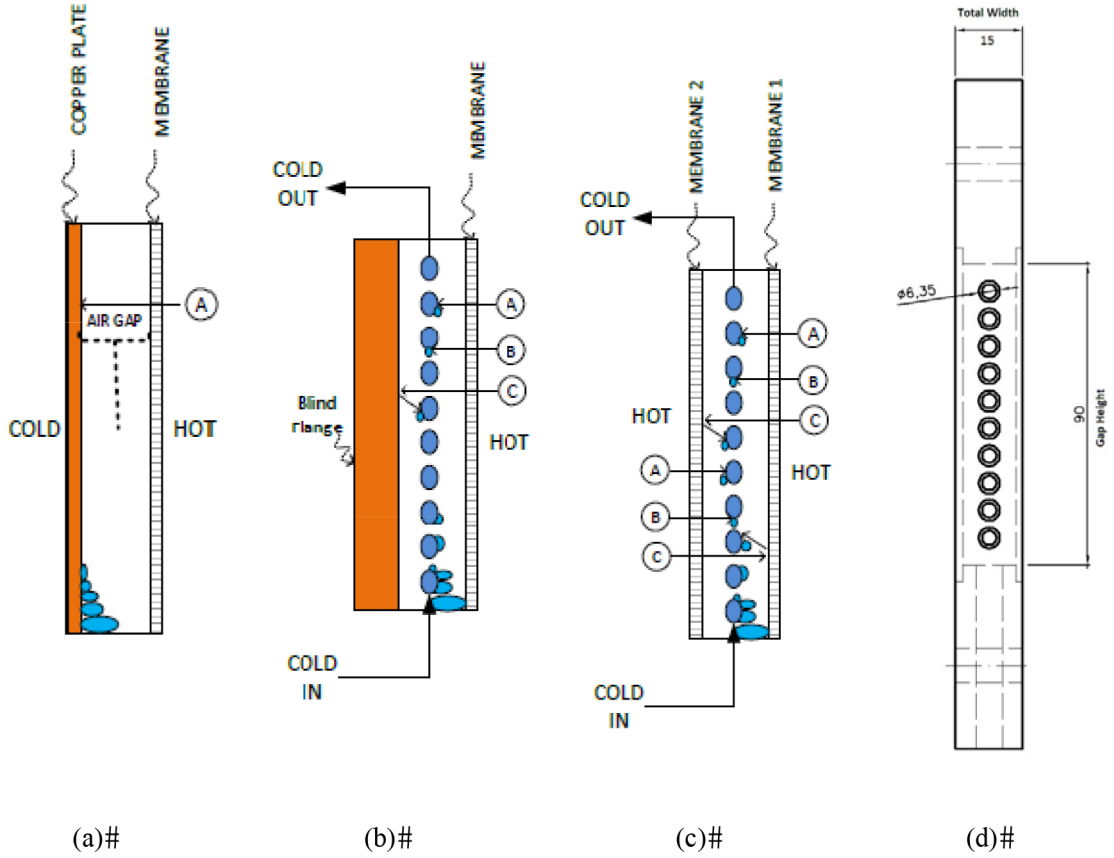

Fig. 6. Equivalent air gaps in different modules; common flat plate condenser (a), tubular condenser with one membrane (b), tubular condenser with two membranes (c), tubular condenser drawing with details (d).

move from both sides of the condenser tubes. The paths of molecules A, B and C will be similar to as Fig. 6b, with the difference that the vapor volume will increase in this case and the collisions of the vapor molecules with condensing tubes occurred more. In this case the probability of vapor collisions with each other will also increase.

According to Fig. 6, the air gap width in case of flat plate condenser is the direct distance between the membrane and the condenser plate, as shown in Fig. 6a. However, the equivalent air gap in a tubular condenser can be obtained by calculating the total surface area of the condenser minus the occupied surface by the tubes shown in Fig. 6b.

$$Air\,Gap\,Width = \frac{Total\,Area - Tubes\,Area}{Gap\,Height} \quad (1)$$

As calculated in Appendix 1, the width of the air gap for tubular condenser is equivalent to 12 mm approximately when using a flat plate condenser. This value will be used in the following sections to compare the efficiency of the tubular condenser with the flat plate condenser.

In all experiments, feed at different temperatures of 40, 50, 60, 70 and 80°C was entered into the module and by maintaining the coolant temperature at 20°C and adjusting the amount of hot and cold circulation flows at 2 L/min, changes in distilled water flux were studied as the only variable parameter in different modules. In order to accurately compare the efficiency of the tube condenser with plate condenser, the equivalent air gap size in the tube condenser was also used in the flat plate condenser. Moreover, the effect of using thin zigzag copper ribbons on the tubular condenser, the effect of membrane pore size, the effect of changes in air gap width and flux variations in the case of using two membranes were investigated. To ensure the results of experiments, each test was repeated three times for all variables.

3. Results and discussion

3.1. Flux in tubular condenser compared with plate type

Fig. 7 shows the distilled water flux values at various temperatures ranging from 40 to 80°C using different condensers. In these experiments the module flux with a flat plate condenser is compared to an ordinary tubular condenser. In this process, the membrane with pore diameter of 0.45 μm was employed. To ensure result's reliability, each test was repeated three times at different temperatures.

According to Fig. 7, the amount of flux of distilled water increases with temperature for both plate and tubular condenser. These graphs show that the amount of distilled water produced by the tubular condenser is greater than that of the flat plate condenser at the same temperatures. For example, at an average temperature of 80°C, the average flux in the case of flat plate condenser is 11.71 kg/m²·h, which increased

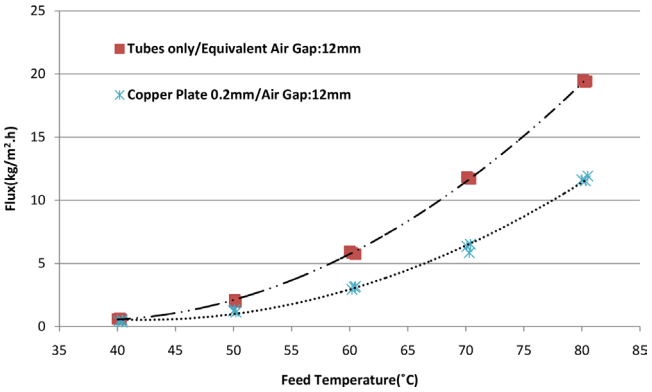

Fig. 7. Comparison of flux in tubular condenser with flat plate condenser.

to 19.45 with a tubular condenser (about 66.3% increase). According to the heat transfer and energy conservation principles (assuming no energy dissipation in the system), the amount of heat transfer due to the condensation of vapors on the flat plate or tube should be provided by the coolant flow through the back of the flat plate or inside the tubes. This heat is equivalent to the heat transferred by the vapor molecules passing through the membrane that entered the module air gap. Using Holman's heat transfer relations for condensation phenomena [52], we have:

$$Q_c = \overline{h}_c A_p (\overline{T}_g - \overline{T}_p) \tag{2}$$

where Q_c is condensation heat transfer rate (W/m²), h_c is heat transfer constant (W/m²·°C), A_p is coolant plate area (m²), $\overline{T}_g$ and $\overline{T}_p$ are the average temperature of the vapors in the air gap and the average temperature of the cooling plate in the half-depth of the plate (°C), respectively. Based on Holman's relations for condensation on a flat plate, the mean value of the constant heat transfer ($\overline{h}$) by integrating along the condensation plate length (L) is obtained by:

$$\overline{h} = \frac{1}{L}\int_0^L h_x dx = \frac{4}{3} h_{x=L} \tag{3}$$

$$\overline{h} = 0.943\left[\frac{\rho(\rho-\rho_g)g h_{fg} {k_f}^3}{L\mu_f (T_g - T_p)}\right]^{\frac{1}{4}} \tag{4}$$

where ρ is the density of water (kg / m³), ρ_g indicates the vapor density (kg/m³), g represents gravity acceleration (m/s²), h_{fg} is enthalpy of vaporization/condensation (J/kg), k_f indicates thermal conductivity of the condensation film (W/m·°C) and μ_f is the dynamic viscosity of condensate film (N·s/m²).

Eq. (4) can be re-stated based on Nusselt's research on the laminar film condensation mode for horizontal tubes:

$$\overline{h} = 0.725\left[\frac{\rho(\rho-\rho_g)g h_{fg} {k_f}^3}{\mu_f d_t (T_g - T_p)}\right]^{\frac{1}{4}} \tag{5}$$

where d_t is the diameter of the tube. Now, if n tubes are parallel to each other, the term nd_t can be replaced by d_t in the above relation [52].

On the other hand, according to the research by Bahar et al. [50], transferred heat during evaporation of saline water from the hot side of the membrane can be expressed as follows (assuming no heat loss):

$$Q_v = \left(\frac{k_{eff} A_m}{t_m} + N c_{pg}\right)(T_m - T_{am}) + N h_{fg} \tag{6}$$

Eq. (6) implies that total heat transfer at the interface (Q_v) is a summation of sensible heat transferred with vapors and latent heat of vaporization. In the above equation, k_{eff} (W/m·°C) is the effective thermal conductivity of the membrane, which includes the thermal conductivity of the membrane and vapors inside the pores, A_m (m²) indicates the membrane area, t_m (m) is the membrane thickness, N represents permeate flux (kg/m²·h), c_{pg} is the specific heat of the vapor (kJ/kg·°C), T_m (°C) is the temperature of the membrane surface that contacts with feed, T_{am} (°C) is the temperature of the membrane surface in contact with the vapor, and h_{fg} is enthalpy of vaporization (J/kg). By rewriting the above relation, we can reach:

$$N = \frac{Q_v - \frac{k_{eff} A_m}{t_m}(T_m - T_{am})}{c_{pg}(T_m - T_{am}) + h_{fg}} \tag{7}$$

It is seen from Eq. (7), if all other parameters are kept constant, Q_v is the determining factor for the evaporation rate. According to the energy conservation principles (no heat loss), heat transfer rate of vaporization is equal to condensation rate, hence: $Q = Q_c = Q_v$.

Therefore the value of N can also be increased by increasing Q_v in Eq. (7) or increasing Q_c in Eq. (2). With substituting Q_c from Eq. (2) instead of Q_v in Eq. (7), we reach:

$$N = \frac{\left[\overline{h}_c A_p\left(\overline{T}_g - \overline{T}_p\right)\right] - \left[\left(\frac{k_{eff} A_m}{t_m}\left(T_m - T_{am}\right)\right)\right]}{c_{pg}\left(T_m - T_{am}\right) + h_{fg}} \tag{8}$$

According to Eq. (8), for a plate condenser, permeate flux will be increased by increasing the condensation surface A_p or increasing the h_c. Therefore, by manipulating the amount of condensation surface, the flux rate can also be affected.

On the other hand, for a tubular condenser, h_c from Eq. (5) can be replaced into Eq. (8):

$$N = \frac{\left\{0.725\left[\frac{\rho(\rho-\rho_g)g h_{fg} {k_f}^3}{\mu_f d_t (T_g - T_p)}\right]^{\frac{1}{4}} A_t\left(\overline{T}_g - \overline{T}_t\right)\right\} - \left\{\left(\frac{k_{eff} A_m}{t_m}\left(T_m - T_{am}\right)\right)\right\}}{c_{pg}\left(T_m - T_{am}\right) + h_{fg}} \tag{9}$$

where A_t (m²) indicates the external surface of the tubes and T_t (°C) is the tube surface temperature. According to Eq. (9), by increasing the external surface of the tubes as condensation surface A_t, permeate flux will be increased.

As calculated in Appendix 2, the condensation heat transfer surface on a flat square plate with a length of 90 mm is 8100 mm². This value in the tubular condenser is increased to 17945 mm². It can be considered that the condensation area of copper tubes is about 2.2 times the flat plate condenser. But according to Eq. (9), condensation area only enhances the first term of equation and other terms

decrease the flux. However, due to the higher thickness of the tubes used in the tubular module than the flat copper plate in plate condenser, it can be expected that the amount of heat transfer in the tubular condenser is lower than the predicted one. In the tubular condenser experiments, with increasing the condensation area to 2.2 times compared to plate one, the flux enhanced only about 66.3%.

It has been reported in [50,51] that using a finned plate instead of a flat plate, the flux increases with an increase in the area. These findings are consistent with the results obtained in this section. They emphasize that increasing the condensation rate creates more free space for vapors and actually creates a "low pressure zone" on the condensation plate, which allows a higher vapor flow rate through the membrane without the need for a change in the feed temperature or change in air gap width. Previously, the use of finned surfaces to increase condensation heat transfer had been studied by Gregorig [45], Fuji et al. [46], Murry et al. [47] and Park [48], where all of them agree on the improvement of condensation heat transfer using finned surface.

3.2. Air gap width impact

The quantities of distilled water flux at different temperatures varying from 40 to 80°C for a 0.45-μm membrane are shown in Fig. 8. In this case a flat plate condenser with two different air gap width, namely; 6-mm and 12-mm compared to the tubular condenser. For the sake of reliability, each test was repeated three times at different temperatures.

According to Fig. 8, distilled water flux increases with the temperature for all three modules. These graphs show that at the same temperatures, the amount of flux produced by the tubular type condenser is greater than the flat plate condenser in both 12 and 6 mm air gap width. Based on the charts, the amount of flux in the case of flat plate condenser increases with the decrease in the air gap width. Comparison of the results shows that, at 80°C, the average flux for flat plate condenser with an air gap of 12 mm is 11.70 kg/ m^2·h. In case of flat plate condenser with an air gap of 6 mm the average flux is 14.34 kg/m^2·h, whereas using tubular condenser, the flux increases to 19.45 kg/m^2·h.

Increasing the air gap width increase the resistance to mass transfer by increasing the vapor diffusion path length. Air molecules in the air gap act as a barrier against the path of vapor molecules that traverse between membrane and condenser plate. Therefore, according to the presented analyses and the experimental results in Fig. 8, it can be stated that the flux ratio is inversely proportional to the air gap width. Analyzing the effect of air gap width in many researches emphasizes that air gap width increasing in the AGMD method is one important factor which reduces the amount of flux significantly [1–2,26].

3.3. Effect of zigzag ribbon on the flux in a tubular condenser

Fig. 9 shows system water flux at various temperatures ranging from 40 to 80°C using three different condensers. In this Figure for a 0.45 μm membrane pore size the flux of a common tubular condenser was compared with two new tubular condenser using 3 and 6 thin copper zigzag ribbon plates. The extended surface area by ribbons are presented in Appendix 3. One ribbon with 10 mm width improve the condensation area about 630 mm^2. For tubular condenser with 3 and 6 ribbons, the condensation area is extended about 1890 and 3780 mm^2 respectively. Again, each test was repeated three times at different temperatures.

According to Fig. 9, flux increases with the temperature for all three modes. These charts show that the use of thin copper ribbon plates on tubular condenser increases the flux in comparison to the common tubular mode and with an increase in the number of thin copper ribbons on tubes from 3 to 6, flux increases significantly. The results indicate that, at 80°C, the average flux in the case of using a condenser with tubes only, is 19.45 kg/m^2·h, while using 3 ribbons, the flux value increased to 22.86 kg/m^2·h, (17.5% increase) and in the case of using 6 ribbons on the condenser, the flux value was enhanced by 54.7% to 30.08 kg/m^2·h.

As shown in Fig. 10a, in the tubular mode without ribbons, some vapor molecules pass through the tubes and the condensation rate decreases, but in case of thin copper ribbon plates, as shown in Fig. 10b, only C and D molecules will travel longer while other molecules will have a shorter path and more points for condensation. When the number of ribbons increased from 3 to 6, the condensation area extended about 1890 and 3780 mm^2 respectively that resulting in more flux. In fact, by increasing the copper ribbon plates, according to Eq. (2), the heat transfer surface 'A' is increased in the equation, and as a result of the condensation area increases, the amount of flux is eventually

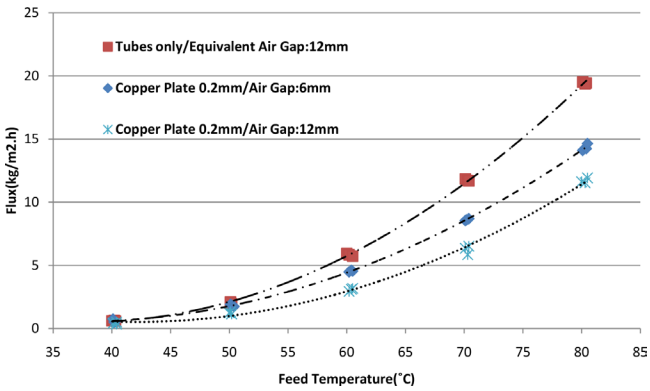

Fig. 8. Flux for flat plate condenser with two different air gap width comparison with tubular condenser.

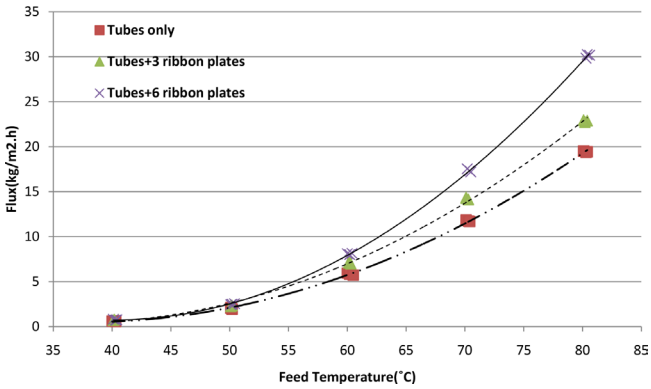

Fig. 9. Effect of zigzag ribbon on the flux in a tubular condenser.

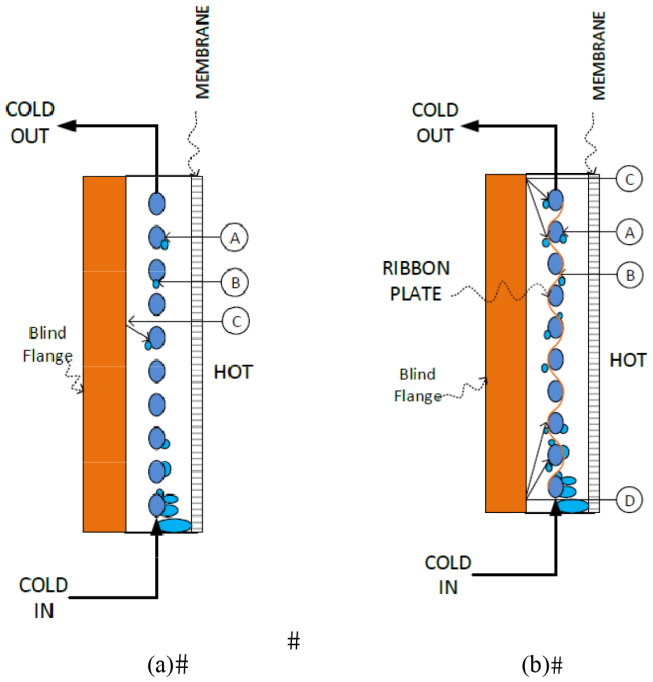

Fig. 10. Using copper ribbon plates on tubular condenser; without ribbon (a), with zigzag ribbons (b).

improved. Using new ribbon configurations other than zigzag or spiral, with the aim of adding to the amount of surface, requires more research.

3.4. Flux variations using two hot-flow chambers on both sides of the developed tubular condenser

Fig. 11 shows system water flux values at various temperatures, from 40 to 70°C, for a developed tubular condenser with 6 ribbon plates using dual membranes (with 0.45 µm pore size) on the both sides of the condenser (two membrane surface = 16200 mm²) in comparison with a single membrane (surface of a membrane = 8100 mm²). To ensure reliability, each test was repeated three times at different temperatures.

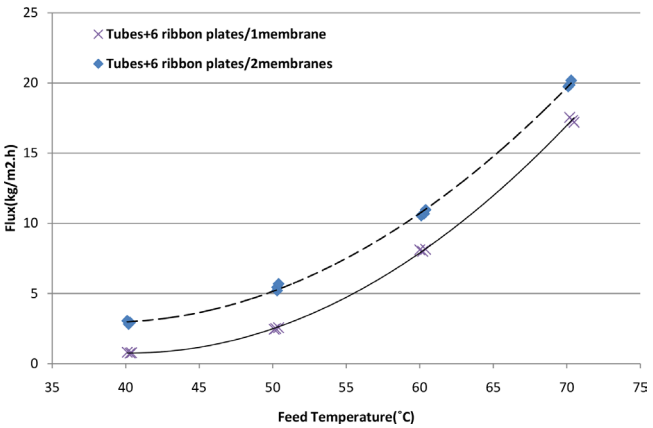

Fig. 11. Flux variations using dual membranes with a developed tubular condenser.

According to Fig. 11, produced distilled water increased with the temperature for both single membrane and dual membranes. These charts illustrate that the amount of flux by two membranes is more than a single membrane at the same temperatures. The results show that at a feed temperature of 70°C, the average flux in the single membrane case is 17.36 kg/m²·h, which increased to 19.93 kg/m²·h for the dual membrane mode.

This increase in flux may be meaningful or is caused due to operating conditions. The justification of these results needs more researches, but we tried to explain the condensation phenomena by Fig. 12. Two main parameters influence the flux; first, membrane surface area and second, a condensation improvement. For calculation of flux with 2 membranes, we divided the total collected permeate to 2 surface area (membrane area = 2*90 mm*90 mm) so the membrane surface area deleted from affecting factors. When we use two membranes, the distance between vapor molecules on both sides of condenser and condensing point is decreased and passed distances for vapor molecules are shorter than the case with one membrane. Also the rate of condensation, which is the number of water molecules that change phase from gas to liquid per second, depends mainly on the vapor pressure. The higher the vapor pressure, the faster the rate of condensation. When we use two membranes, the number of steam molecules in condensation chamber is increased. An increase in the number of vapor molecules leads to an increase in collision and interactions among molecules and also increases the condensation chamber's pressure.

In Fig. 12 the condensation phenomena for a developed tubular condenser using one or two membranes in the mod-

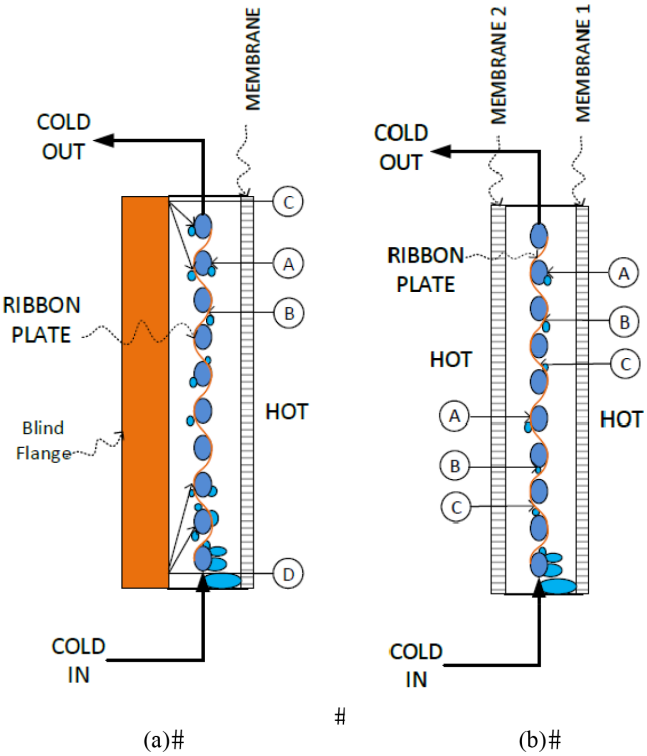

Fig. 12. Schematic of condensation with a developed tubular condenser; single membrane (a), dual membranes (b).

ule has been compared. In a single membrane mode shown in Fig. 12a, vapor molecules A and B collide with tubes and ribbon plates, but molecules C and D must travel longer distances behind the tubes and ribbon plates for condensing there. In addition, the amount of produced vapors is lower, while in the dual mode in Fig. 12b, the produced vapors on both sides of the condenser are larger by two membranes and the distance traveled to collide with the condenser decreases for the molecules, hence the condensation rate is higher and the amount of flux is increased.

In case of using two membranes and up to a temperature of about 70°C, the cooling temperature of the coolant fluid remains constant at 20°C due to the limited cooling capacity of chiller used in these tests and therefore, the results of the above diagram are obtained. But with the temperature rising up to 80°C, this chiller is not able to provide the optimal cooling for the condensation of vapors passing through dual membranes, and as a result, the temperature of the cold fluid rises from 20°C to about 32°C. Therefore, the flux results at temperatures above 70°C cannot be measured.

An increase in the amount of flux owing to the increase in the membrane surface area, while the condenser capacity is unchanged, indicates that more vapors have a condensing capability with the existing cooling capacity. Therefore, at temperatures below 70°C, the existing cooling capacity increases the amount of the total flux. However, this increase is stopped at the temperatures above 70°C due to overcoming vaporization heat to chiller's cooling potential.

3.5. The effect of membrane pore size

Fig. 13 illustrates the produced fluxes in two modes of flat plate condenser and developed tubular condenser at various temperatures ranging from 40 to 80°C for two different membrane pore sizes: 0.22 and 0.45 µm. To ensure reliability, each test was repeated three times at different temperatures.

According to Fig. 13, the amount of produced distilled water is increased by an increase in the pore size of the membrane. Also charts show that in both types of membranes, with an increase in the feed temperature, the flux of produced distilled water increased too. Based on the results, at 80°C, the mean flux in the case of a 0.45 µm membrane for a developed tubular condenser is 30.08 kg/m²·h, where it decreases to 27.10 for a membrane with 0.22 µm pore size (about 11% reduction). Also, at the same temperature, for a membrane with a pore size of 0.45 microns with the flat plate condenser, the flux is 11.70 kg/m²·h which decreased to 9.49 kg/m²·h for the membrane with 0.22 micron pore size (23.8% reduction).

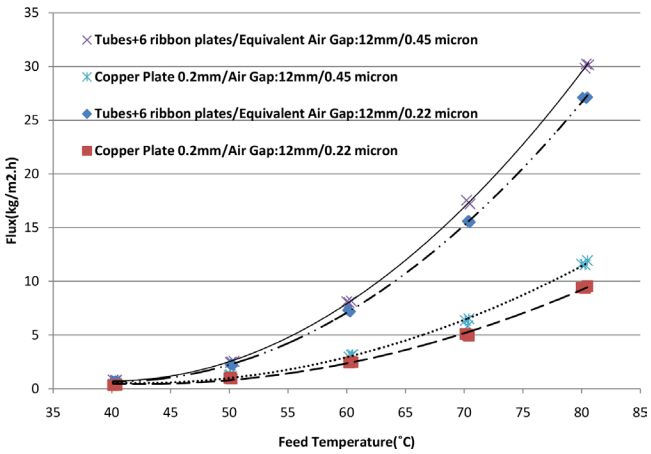

Fig. 13. The effect of membrane pore size on the permeate flux.

The transfer of vapor molecules through the structure of the porous membrane takes place by varying the vapor pressure of the two sides of the membrane. According to information provided in various references, mass flux depends directly on the difference in water vapor pressure on the membrane (Δpi) and mass transfer constant (C) [1–4].

$$N = C\Delta p_i \tag{10}$$

Simplification of the constant mass transfer equations shows the general dependence of the mass transfer on the properties of the membrane:

$$C \sim \frac{\varepsilon r^{\alpha}}{\tau t_m} \tag{11}$$

In Eq. (11), ε is the membrane porosity, r is the mean radius of the pores, τ is the membrane's tortuosity, t_m is the membrane thickness, and α is diffusion type coefficient [53].

According to Eq. (11), the mass transfer constant is directly related to membrane pore size and with an increasing average radius of the membrane pores, the amount of produced flux will increase. On the other hand, by increasing the feed temperature, the difference between the water vapor pressure on the membrane (Δpi) in Eq. (10) increases and eventually increases the amount of flux (N).

Increasing the amount of flux with increasing temperature and increasing the size of the membrane pores have been emphasized in many previous studies which is consistent with the results obtained in this research [1–2,26–27,54–55].

3.6. Gained output ratio (GOR)

Gained output ratio (GOR) is defined as a ratio between mass flow rate of produced distillate (m_d) and mass flow rate of saturated steam (m_s) [56].

$$GOR = \frac{m_d}{m_s} \tag{12}$$

The factor m_d in Eq. (12) is the amount of distillate (kg) whereas m_s is defined as:

$$m_s = \frac{m_h C_p \left(T_{h,out} - T_{h,in}\right)}{\Delta H_{ref}} \tag{13}$$

That in Eq. (13) m_h is the mass flow rate of hot fluid (kg/h), C_p is the specific heat capacity(kJ/kg·K), $T_{h,out}$ and $T_{h,in}$ are outlet and inlet temperature of feed fluid (°C) and ΔH_{ref} is the latent heat of steam at standard conditions (1 atm and 100°C) that has a value of 2326 kJ/kg [57].

Fig. 14 illustrates the GOR using Eq. (12) and Eq. (13) for three types of condensers that presented in experiments;

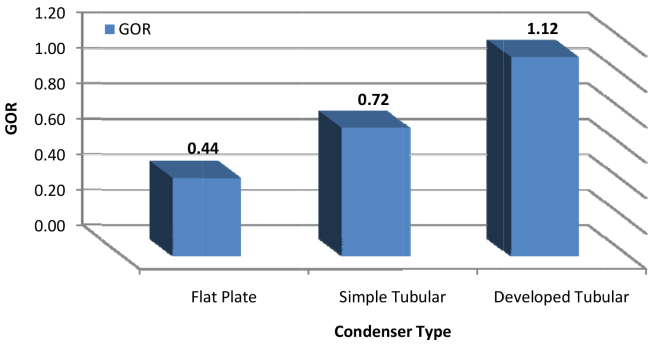

Fig. 14. Gained output ratio(GOR) for three different types of condensers; flat plate condenser, simple tubular condenser and developed tubular condenser.

flat plate condenser, simple tubular condenser and developed tubular condenser with zigzag ribbons.

According to Fig. 14, the GOR for flat plate condenser is 0.44. This value is enhanced about 65% with substituting the simple tubular condenser instead of the flat plate type. With replacement of developed tubular condenser, the GOR is increased to 1.12 that shows 156% improvement. In some researches, GOR for AGMD process is reported from 0.8–0.97 [58–60]. The GOR for developed tubular condenser indicates 15% improvement compared with other researchers results.

3.7. Salt rejection rate (SRR)

Salt rejection rate (SRR) is an important factor for investigation of MD module efficiency. The salt rejection is difference between initial feed concentration (C_{feed}) and produced distillate concentration ($C_{distillate}$) that is defined using Eq. (14):

$$SRR = \frac{C_{feed} - C_{distillate}}{C_{feed}} * 100 \quad (14)$$

Fig. 15 illustrates the rejection rate for three different condensers using Eq. (14).

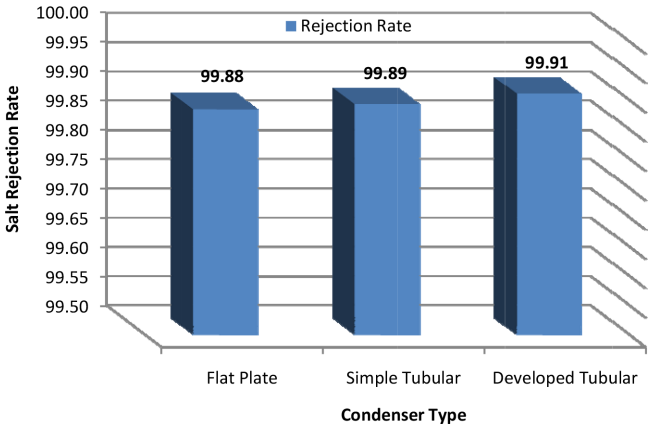

Fig. 15. Rejection rate for three different types of condensers; flat plate condenser, simple tubular condenser and developed tubular condenser.

4. Conclusions

Due to the increasing attention of the researchers to the membrane distillation (MD) technology and the abundant demand for this process, improving the performance of MD by the new configurations' presentation is needed urgently. In this research with the aim of improving the condensation phenomenon and consequently, enhancing the efficiency of AGMD process, a new module configuration was proposed. In this new module, with replacing horizontal copper tubes instead of a flat coolant plate, a tubular condenser was introduced. Using two types of PTFE commercial flat sheet membranes, laboratory prepared brackish water was introduced into the system at different temperatures, and by setting the coolant temperature at 20°C and adjusting the flow rate of hot and cold currents to 2 liters per minute, changes in distilled water flux were studied. According to the results, the average flux of the new tubular module indicated 66% improvement compared with the common flat plate condenser. Furthermore, by adding thin copper ribbons to the tubular condenser, the flux increased up to 30.08 kg/(m²·h) that in comparison with the conventional flat plate condenser, represents an enhancement of about 160%. Increasing the condensation area, the feed temperature and membrane pore size and decreasing air gap width caused flux improvement that emphasized this new arrangement matched with other configurations results. Other advantages of using this new tubular condenser include the ability to use two membranes on both sides of tubular condenser instead of a single membrane, decreasing module size, greater flexibility of the process and the possibility of reducing energy consumption in the condensation section. The maximum flux by using two membranes in a module with a new developed tubular condenser by zigzag ribbons is about 15% higher than a single membrane mode. Moreover, by adding a 160% improvement in single-membrane mode to a conventional flat plate condenser, 175% of the overall flux improvement was achieved in the case with two membranes. The results demonstrated that the implementation of a developed tubular condenser instead of a flat coolant plate can be an effective way to enhance the efficiency of AGMD process. Developing this new configuration with new suggestions for improving the condensation needs more research. Proposing another sheet configuration, using finned tubes and new offers for air gap reduction can be the subject of future research.

Acknowledgement

This research did not receive any specific grant from funding agencies in the public, commercial, or not-for-profit sectors.

Symbols

A_m	—	Membrane surface area (m²)
A_p	—	Coolant plate area (m²)
A_t	—	The external surface of the tubes (m²)
C	—	Mass transfer constant
C_p	—	The specific heat capacity (kJ/kg·K)
c_{pg}	—	The specific heat of the vapor (kJ/kg·°C)

d	—	Diameter of the pores (m)
d_t	—	Diameter of the tubes (m)
g	—	Gravity acceleration (m/s^2)
h	—	Constant heat transfer (W/m^2·°C)
h_c	—	Heat transfer constant of convection (W/m^2· °C)
h_{fg}	—	Enthalpy of vaporization/condensation (J/kg)
k_{eff}	—	The effective thermal conductivity of the membrane (W/m· °C)
k_f	—	Thermal conductivity of condensation film (W/m· °C)
L	—	Condensation plate length (m)
m_d	—	Amount of distillate (kg)
m_s	—	Amount of saturated steam (kg)
m_h	—	Amount of hot fluid (kg)
M	—	Molar weight (kg/mole)
N	—	Permeate mass flux (kg/m^2·h)
P	—	Pressure (Pa)
Q	—	Heat transfer rate (W/m^2)
Q_c	—	Condensation heat transfer rate (W/m^2)
Q_v	—	Evaporation heat transfer rate (W/m^2)
r	—	The mean radius of the pores (m)
T	—	Temperature (K)
T	—	Time (s)
T_{am}	—	The temperature of the membrane surface in contact with the vapor (°C)
T_g	—	Average temperature of the vapors in the air gap (°C)
t_m	—	Membrane thickness (μm)
T_m	—	The temperature of the membrane surface (°C)
T_p	—	Average temperature of the cooling plate (°C)
T_t	—	The tube surface temperature (°C)
ΔH_{ref}	—	The latent heat of steam at standard conditions (kJ/kg)
Δp_i	—	The difference in water vapor pressure on the membrane

Greek

α	—	Diffusion constant
ε	—	Porosity (%)
μ	—	Dynamic viscosity (N·s/m^2)
μ_f	—	Dynamic viscosity of condensate film (N·s/m^2)
ρ	—	Density of water (kg/m^3)
ρ_g	—	Vapor density in the air gap (kg/m^3)
τ	—	Tortuosity

References

[1] E. Drioli, A. Ali, F. Macedonio, Membrane distillation: Recent developments and perspectives, Desalination, 356 (2015) 56–84.

[2] P. Wang, T. Chung, Recent advances in membrane distillation processes: Membrane development, configuration design and application exploring, J. Membr. Sci., 474 (2015) 39–56.

[3] M.R. Qtaishat, F. Banat, Desalination by solar powered membrane distillation systems, Desalination, 308 (2013) 186–197.

[4] M. Khayet, Solar desalination by membrane distillation: Dispersion in energy consumption analysis and water production costs, (a review), Desalination, 308 (2013) 89–101.

[5] A. Alkhudhiri, N. Hilal, Air gap membrane distillation: A detailed study of high saline solution, Desalination, 403 (2017) 179–186.

[6] A. Alkhudhiri, N. Darwish, N. Hilal, Treatment of high salinity solutions: application of air gap membrane distillation, Desalination, 287 (2012) 55–60.

[7] A. Alkhudhiri, N. Darwish, N. Hilal, Produced water treatment: application of air gap membrane distillation, Desalination, 309 (2013) 46–51.

[8] I. Janajreh, Kh. El Kadi, R. Hashaikeh, R. Ahmed, Numerical investigation of air gap membrane distillation (AGMD): Seeking optimal performance, Desalination, 424 (2017) 122–130.

[9] A.E. Jansen, J.W. Assink, J.H. Hanemaaijer, J. van Medevoort, E. van Sonsbeek, Development and pilot testing of full-scale membrane distillation modules for deployment of waste heat, Desalination, 323 (2013) 55–65.

[10] J.H. Hanemaaijer, Memstills-low cost membrane distillation technology for seawater desalination, Desalination, 168 (2004) 355.

[11] C. Dotremont, B. Kregersman, R. Sih, K.C. Lai, K. Koh, H. Seah, Sea water desalination with memstill technology - a sustainable solution for the industry, Water Practice Technol., 5 (2009).

[12] http://www.aquastill.nl/Modules.html.

[13] A.M. Islam, Membrane distillation process for pure water and removal of arsenic, in department of materials and surface chemistry, Chalmers University of Technology, Sweden, pp. 35.

[14] Scarab development solution to fabrication plant, in: Water Desalination Report, (2000).

[15] E.K. Summers, H.a. Arafat, J.H. Lienhard, Energy efficiency comparison of single-stage membrane distillation (MD) desalination cycles in different configurations, Desalination, 290 (2012) 54–66.

[16] S. Cerneaux, I. Strużyńska, W.M. Kujawski, M. Persin, A. Larbot, Comparison of various membrane distillation methods for desalination using hydrophobic ceramic membranes, J. Membr. Sci., 337(1–2) (2009) 55–60.

[17] Z. Ding, L. Liu, Z. Li, R. Ma, Z. Yang, Experimental study of ammonia removal from water by membrane distillation (MD): the comparison of three configurations, J. Membr. Sci., 286(1–2) (2006) 93–103.

[18] A.M. Alklaibi, N. Lior, Comparative study of direct-contact and air-gap membrane distillation processes, Ind. Eng. Chem. Res., 46(2) (2007) 584–590.

[19] E. Guillén-Burrieza, J. Blanco, G. Zaragoza, D.-C. Alarcón, P. Palenzuela, M. Ibarra, W. Gernjak, Experimental analysis of an air gap membrane distillation solar desalination pilot system, J. Membr. Sci., 379 (2011) 386–396.

[20] M. Khayet, T. Matsuura, Application of surface modifying macromolecules for the preparation of membranes for membrane distillation flux enhancement in membrane distillation by fabrication of dual layer hydrophilic–hydrophobic hollow fibre membranes, Desalination, 158 (2003) 51–56.

[21] P. Peng, A.G. Fane, X. Li, Desalination by membrane distillation adopting a hydrophilic membrane, Desalination, 173 (2005) 45–54.

[22] M. Khayet, T. Matsuura, J.I. Mengual, M. Qtaishat, Design of novel direct contact membrane distillation membranes, Desalination, 192 (2006) 105–111.

[23] J. Xu, M. Furuswa, A. Ito, Air-sweep vacuum membrane distillation using fine silicone rubber hollow-fiber membranes, Desalination, 191 (2006) 223–231.

[24] S. Bonyadi, T.S. Chung, Flux enhancement in membrane distillation by fabrication of dual layer hydrophilic–hydrophobic hollow fiber membranes, J. Membr. Sci., 306 (2007) 134–146.

[25] C. Feng, K.C. Khulbe, T. Matsuura, R. Gopal, S. Kaur, S. Ramakrishna, M. Khayet, Production of drinking water from saline water by air-gap membrane distillation using polyvinylidene fluoride nanofiber membrane, J. Membr. Sci., 311 (2008) 1–6.

[26] J. Xu, Y.B. Singh, G.L. Amy, N. Ghaffour, Effect of operating parameters and membrane characteristics on air gap mem-

brane distillation performance for the treatment of highly saline water, J. Membr. Sci., 512 (2016) 73–82.
[27] R. Tian, H. Gao, X.H. Yang, S.Y. Yan, S. Li, A new enhancement technique on air gap membrane distillation, Desalination, 332 (2014) 52–59.
[28] D. Wirth, C. Cabassud, Water desalination using membrane distillation: comparison between inside/out and outside/in permeation, Desalination, 147 (2002) 139–145.
[29] C.D. Ho, C.-H. Huang, F.-C. Tsai, W.-T. Chen, Performance improvement on distillate flux of counter current-flow direct contact membrane distillation systems, Desalination, 338 (2014) 26–32.
[30] L. Wang, H. Wang, B. Li, Y. Wang, S. Wang, Novel design of liquid distributors for VMD performance improvement based on cross-flow membrane module, Desalination, 336 (2014) 80–86.
[31] M.N. Chernyshov, G.W. Meindersma, A.B. de Haan, Comparison of spacers for temperature polarization reduction in air gap membrane distillation, Desalination, 183 (2005) 363–374.
[32] L. Chu-Lien, C. Yu-Feng, S. Wen-Junn, W. Chi-Chuan, Introducing flow deflectors effect of flow deflector on the flux improvement in direct contact membrane distillation, Desalination, 253 (2010) 16–21.
[33] M. Shakaib, S.M.F. Hasani, I. Ahmed, R.M. Yunus, A CFD study on the effect of spacer orientation on temperature polarization in membrane distillation modules, Desalination, 284 (2012) 332–340.
[34] F. He, J. Gilron, K.K. Sirkar, High water recovery in direct contact membrane distillation using a series of cascades, Desalination, 323 (2013) 48–54.
[35] X. Yang, R. Wang, A.G. Fane, Novel designs for improving the performance of hollow fiber membrane distillation modules, J. Membr. Sci., 384(1–2) (2011) 52–62.
[36] D. Singh, K.K. Sirkar, Desalination by air gap membrane distillation using a two hollow-fiber-set membrane module, J. Membr. Sci., 421–422 (2012) 172–179.
[37] H. Geng, H. Wu, P. Li, Q. He, Study on a new air-gap membrane distillation module for desalination, Desalination, 334(1) (2014) 29–38.
[38] D. Winter, J. Koschikowski, S. Ripperger, Desalination using membrane distillation: flux enhancement by feed water deaeration on spiral-wound modules, J. Membr. Sci., 423–424 (2012) 215–224.
[39] Y. Qin, Y. Wu, L. Liu, D. Cui, Y. Zhang, D. Liu, K. Yao, Y. Liu, A. Wang, W. Li, Multi-effect membrane distillation process for desalination and concentration of aqueous solutions of non-volatile or semi-volatile solutes, AIChE, Salt Lake City, UT, 2010.
[40] http://www.water-technology.net/news/news-ge-memsys-successfully-test-new-membrane-distillation-system.
[41] G.W. Meindersma, C.M. Guijt, A.B. de Haan, Desalination and water recycling by air gap membrane distillation, Desalination, 187 (2006) 291–301.
[42] G. Hongxin, W. Haoyun, L. Pingli, H. Qingfeng, Study on a new air-gap membrane distillation module for desalination, Desalination, 334 (2014) 29–38.
[43] R. Chouikh, S. Bouguecha, M. Dhahbi, Modelling of a modified air gap distillation membrane for the desalination of seawater, Desalination, 181 (2005) 257–265.
[44] R. Bahar, M.N.A. Hawlader, T.F. Ariff, Effect of coolant plate geometry and material in a freshwater production system: an experimental study, Presented in 2nd International Conference on Advances in Manufacturing and Materials Engineering (ICAMME 2014), Kuala Lumpur Malaysia, September 23–25 (2014).
[45] R. Gregorig, Hautkondensation an feingewellten Oberflächen bei Berücksich-tigung der Oberflächenspannungen, Zeitschrift für Angewandte, Math. Phys. (ZAMP), 5(1) (1954) 36–49.
[46] T. Fujii, H. Honda, Laminar film condensation on a vertical single fluted plate, Proceedings of the Sixth International Heat Transfer Conference, 2 (1978) 419–424.
[47] Y. Mori, K. Hijikata, S. Hirasawa, W. Nakayama, Optimized performance of condensers with outside condensing surfaces, J. Heat Transf. Trans., ASME, 103(2) (1981) 96–102.
[48] I.S. Park, Numerical analysis for flow, heat and mass transfer in film flow along a vertical fluted tube, Int. J. Heat Mass Transf., 53 (2010) 309–319.
[49] Zh. Liu, Q. Gao, X. Lu, L. Zhao, S. Wu, Zh. Ma, H. Zhang, Study on the performance of double-pipe air gap membrane distillation module, Desalination, 396 (2016) 48–56.
[50] R. Bahar, M.N.A. Hawlader, T.F. Ariff, Channeled coolant plate: A new method to enhance freshwater production from an air gap membrane distillation (AGMD) desalination unit, Desalination, 359 (2015) 71–81.
[51] M.J.P. Bappy, R. Bahar, Sh. Ibrahim, T.F. Ariff, Enhanced freshwater production using finned-late air gap membrane distillation (AGMD), MATEC Web of Conferences, 103 (2017) 06014.
[52] J.P. Holman, Heat transfer, 10th Edition McGraw-Hill, New York, 2010.
[53] L. Eykens, K. De Sitter, C. Dotremont, L. Pinoy, B. Van der Bruggen, How to optimize the membrane properties for membrane distillation: A Review, Ind. Eng. Chem. Res., 55 (2016) 9333–9343.
[54] R.M.A. Roque-Malherbe, Adsorption and diffusion in nanoporous materials, CRC press, Taylor & Francis Group, Florida, 2007.
[55] A. Khalifa, D. Lawal, M. Antar, M. Khayet, Experimental and theoretical investigation on water desalination using air gap membrane distillation, Desalination, 376 (2015) 94–108.
[56] A.K. Fard, Y.M. Manawi, T. Rhadfi, K.A. Mahmoud, M. Khraisheh, F. Benyahia, Synoptic analysis of direct contact membrane distillation performance in Qatar: A case study, Desalination, 360 (2015) 97–107.
[57] C. Summariva, Desalination in the gulf, International Desalination Association (IDA), Perugia, (2011).
[58] E. Guillen-Burrieza, J. Blanco, G. Zaragoza, D.C. Alarcon, P. Palenzuela, M. Ibarra, W. Gernjak, Experimental analysis of an air gap membrane distillation solar desalination pilot system, J. Membr. Sci., 379 (2011) 386–396.
[59] H.E. Fath, S.M. Elsherbiny, A.A. Hassan, M. Rommel, M. Wieghaus, J. Koschikowski, M. Vatansever, PV and thermally driven small-scale, stand-alone solar desalination systems with very low maintenance needs, Desalination, 225 (2008) 58–69.
[60] F. Banat, Desalination by a "compact SMADES" autonomous solar-powered membrane distillation unit, Desalination, 217 (2007) 29–37.

Appendix 1: Equivalent air gap in tubular condenser

$$Air\,Gap\,Width = \frac{Total\,Area - Tubes\,Area}{Gap\,Height} \quad (1)$$

As shown in Fig. 6d, the total surface area is calculated as the product of the air gap length (90 mm) and in the condenser width (15 mm).

Total area = Gap height * Total width = 90 mm * 15 mm = 1350 mm^2

The area occupied by the tubes is calculated as the product of the surface of a tube with an external diameter of 1/4 inches (6.35 mm) and the total number of tubes (10 tubes).

Tubes area = Area of one tube ($\pi d^2/4$) * No. of tubes = (3.14 * $(6.35)^2/4$) * 10 = 316.53 mm^2

By establishing the air gap height (90 mm) and putting the computed values above in Eq. (1), an equivalent air gap is obtained.

Equivalent air gap width = (1350 mm^2 – 316.53 mm^2) / 90 mm = 11.48 mm

Appendix 2: Condensation heat transfer surface

The condensation heat transfer surface on a flat plate in the form of a square with a length of 90 mm is:

$A_{flat\ plate}$ = 90 mm * 90 mm = 8100 mm^2

This value in the tubular condenser will be equal to the summation of the outer surfaces of all tubes. Hence, we have:

$A_{Tubes} = n * (\pi * d) * L$

The number of tubes used in the condenser is 10, the outer diameter of the tubes is 6.35 mm, and the length of each branch of the tube is 90 mm. By substituting these values into the equation above, the area of all the tubes will be:

$A_{Tubes} = n * (\pi * d) * L = 10 * 3.14 * 6.35 * 90 = 17945.1\ mm^2$

Appendix 3: Condensation surface for tubular condenser with ribbons

Copper ribbons of 0.2 mm thickness were used in the form of a zigzag in two modes, including; 3 ribbons for half the tubes, shown in Fig. 2b, and 6 ribbons for covering the total surface of the tubes that is illustrated in Fig. 2c. The width of a ribbon is 10 mm. The ribbon length between two tubes is 3.5 mm. Total length of ribbon among the 10 tubes is:

9*3.5=31.5 mm Area added by a ribbon= 31.5*10=315 mm^2

Both sides of ribbon are employed as condensation area:

Total area added by a ribbon = 315*2 = 630 mm^2
For 3 ribbons: Total added area = 3*630 = 1890 mm^2
For 6 ribbons: Total added area = 6*630 = 3780 mm^2